Mechanism of Ba^{2+} Block of M-like K Channels of Rod Photoreceptors of Tiger Salamanders

LONNIE P. WOLLMUTH

From the Department of Physiology and Biophysics, University of Washington School of Medicine, Seattle, Washington 98195

ABSTRACT I_{Kx} is a voltage-dependent K^+ current in the inner segment of rod photoreceptors that shows many similarities to M-current. The depression of I_{Kx} by external Ba^{2+} was studied with whole-cell voltage clamp. Ba^{2+} reduced the conductance and voltage sensitivity of I_{Kx} tail currents and shifted the voltage range over which they appeared to more positive potentials. These effects showed different sensitivities to Ba^{2+}: conductance was the least sensitive ($K_{0.5}$ = 7.6 mM), voltage dependence intermediate ($K_{0.5}$ = 2.4 mM) and voltage sensitivity the most sensitive ($K_{0.5}$ = 0.2 mM). Ca^{2+}, Co^{2+}, Mn^{2+}, Sr^{2+}, and Zn^{2+} did not have actions comparable to Ba^{2+} on the voltage dependence or the voltage sensitivity of I_{Kx} tail currents. In high K^+ (100 mM), the voltage range of activation of I_{Kx} was shifted 20 mV negative, as was the τ-voltage relation. High K^+ did not prevent the effect of Ba^{2+} on conductance, but abolished its ability to affect voltage dependence and voltage sensitivity. Ba^{2+} also altered the apparent time-course of activation and deactivation of I_{Kx}. Low Ba^{2+} (0.2 mM) slowed both deactivation and activation, with most effect on deactivation; at higher concentrations (1–25 mM), deactivation and activation time courses were equally affected, and at the highest concentrations, 5 and 25 mM Ba^{2+}, the time course became faster than control. Rapid application of 5 mM Ba^{2+} suggested that the time dependent currents in Ba^{2+} reflect in part the slow voltage-dependent block and unblock of I_{Kx} channels by Ba^{2+}. This blocking action of Ba^{2+} was steeply voltage-dependent with an apparent electrical distance of 1.07. Ba^{2+} appears to interact with I_{Kx} channels at multiple sites. A model which assumes that Ba^{2+} has a voltage-independent and a voltage-dependent blocking action on open or closed I_{Kx} channels reproduced many aspects of the data; the voltage-dependent component could account for both the Ba^{2+}-induced shift in voltage dependence and reduction in voltage sensitivity of I_{Kx} tail currents.

INTRODUCTION

I_{Kx} is a time- and voltage-dependent K^+ current identified in the inner segment of tiger salamander rod photoreceptors that plays an important role in shaping the waveform of the receptor potential in response to dim flashes of light (Attwell and

Address correspondence to Dr. Lonnie P. Wollmuth, Department of Physiology and Biophysics, SJ-40, University of Washington School of Medicine, Seattle, WA 98195.

J. GEN. PHYSIOL. © The Rockefeller University Press · 0022-1295/94/01/0045/22 $2.00
Volume 103 January 1994 45–66

Wilson, 1980; Beech and Barnes, 1989). This conductance shares many features with the M-current (I_M) first described in sympathetic neurons (Adams, Brown, and Constanti, 1982*a, b*), including a comparable voltage range of activation, slow gating kinetics, no inactivation or obvious delay in activation and only a weak sensitivity to tetraethylammonium and 4-aminopyridine. It differs in that it is not suppressed by muscarinic agonists, probably because rods lack the proper muscarinic receptors. Hence, in NG108-15 cells, a neuroblastoma x glia cell line containing endogenous m4-muscarinic receptors, an M-like current is not modulated by muscarine until the cells are transfected with either m1- or m3-receptors (Robbins, Caulfield, Higashida, and Brown, 1991).

Many K^+ currents, including I_{Kx} and I_M, are reduced by external Ba^{2+} (Hagiwara, Miyazaki, Moody, Patlak, 1978; Eaton and Brodwick, 1980; Armstrong and Taylor, 1980; Adams et al., 1982*b;* Vergara and Latorre, 1983; Beech and Barnes, 1989; Robbins, Trouslard, Marsh, and Brown, 1992). For many K channel types, the mechanism of action of Ba^{2+} appears to be a direct plugging of the pore that is removed by depolarization (e.g., Armstrong and Taylor, 1980). For I_{Kx} and other M-like channels, the action of Ba^{2+} appears complex (Beech and Barnes, 1989; Robbins et al., 1992). It may interact with the channel at multiple sites, and if Ba^{2+} plugs the pore in a voltage-dependent manner, the rate of Ba^{2+} block and unblock is remarkably similar to the time course of I_{Kx} gating. Alternatively, the similarity in time course of currents in the presence and absence of Ba^{2+} may reflect that Ba^{2+} interacts with the gating machinery of I_{Kx} channels either directly or allosterically shifting strongly positive the voltage-dependence of I_{Kx} gating. Here I investigated how Ba^{2+} and other divalents affected the gating and time-dependence of I_{Kx} and looked for interaction between Ba^{2+} and K^+ to dissect out how Ba^{2+} interacts with I_{Kx} channels and to develop a quantitative model to describe this interaction.

MATERIALS AND METHODS

Isolation of Rod Photoreceptors

Rod photoreceptors were isolated from the retina of aquatic tiger salamanders (*Ambystoma tigrinum;* Kons Scientific Co., Inc., Germantown, WI). Salamanders were maintained at room temperature with ambient illumination for at least 24 h before experimentation. An animal was decapitated, the head was hemisected, and the eyeballs were removed. The retina was isolated from the eyeball and a cell suspension was made by triturating the retina in Ringer's solution using a cut-off, fire-polished Pasteur pipette. Recordings were made from solitary rods under constant bright light from the microscope illuminator.

Solutions

External. The Cs/Cd Ringer's external solution was designed to emphasize I_{Kx} (mM): 90 NaCl; 2.5 KCl; 3 $CaCl_2$; 8 glucose; 10 HEPES; 5 CsCl; 0.1 $CdCl_2$; pH adjusted to 7.4 with NaOH. I_{Kx} appears insensitive to external Cs^+ and Cd^{2+} (see Fig. 1, Beech and Barnes, 1989). In a few experiments, Ca^{2+} was omitted. In other solutions, the KCl was raised to 5, 10, or 20 mM. For the 100 mM K^+ solution, 90 mM NaCl and 2.5 mM KCl were replaced by 100 mM KCl. All divalent cations tested, as well as tetraethylammonium (TEA), were added without substitution.

Internal. The pipette solution was (mM): 80 KCl; 20 NaCl; 3.5 $MgCl_2$; 10 HEPES; 1 EGTA; 1.5 ATP; 0.1 GTP; pH adjusted to 7.4 with KOH. EGTA and ATP were obtained from

Sigma Chemical Co. (St. Louis, MO), GTP from P-L Biochemicals (Milwaukee, WI) and HEPES was from Calbiochem Corp. (La Jolla, CA).

Whole-Cell Recording

The whole-cell version of the patch clamp technique (Hamill, Marty, Neher, Sakmann, and Sigworth, 1981) was used to voltage-clamp and dialyze cells at room temperature (21–24°C). Electrodes were pulled from glass hematocrit tubes (VWR Scientific Corp., Seattle, WA) and had resistances of 2–5 MΩ when measured in the Cs/Cd Ringer's and the standard internal solution. The pipette was sealed to the inner segment of the photoreceptor, the patch was broken by suction, and whole-cell membrane current was measured using an Axopatch 1-C Patch Clamp (Axon Instruments Inc., Foster City, CA). Currents were recorded with partial pipette and membrane capacitance compensation, low-pass filtered at 200 Hz, digitized at 1 kHz, and stored and analyzed on an IBM-compatible computer using the BASIC-FASTLAB software and hardware package (INDEC Systems Inc., Capitola, CA). Boltzmann, Hill and linear equations were fitted using nonlinear least squares. Results are reported as mean ± SEM.

The recording chamber consisted of three connected wells cut out from a layer of Sylgard at the bottom of a Petri dish. Cell suspensions were pipetted into the center and largest well (100–200 μl). The two end chambers were the inflow and outflow for superfusion. For all experiments, solution flow was continuous. In some experiments, solutions were rapidly exchanged in addition to the normal continuous superfusion with Cs/Cd Ringer's (see Bernheim, Beech, and Hille, 1991). Solution flow was rapidly switched between the two halves of a theta tube (Clark Electromedical Instruments, Reading, England) by computer-controlled solenoid valves. One half of each theta tube contained Cs/Cd Ringer's while the other half contained either 20 mM K^+ or 5 mM Ba^{2+}. Rapid application measurements were used only when the decrease in outward current was well described by a single exponential and were uniform with repeated applications.

Liquid-junction potentials measured using a Beckman ceramic-junction, saturated-KCl electrode were corrected for during data analysis. The junction potential between the Cs/Cd Ringer's and the standard pipette solution was −2 mV (pipette negative). Adding $BaCl_2$ to the Cs/Cd Ringer's generated junction potentials at the ground electrode of 1 mV (5 mM), 3 mV (25 mM), and 4 mV (50 mM) (ground electrode 0 mV). Voltage protocols in the figure legends describe potentials only for 0 Ba^+, Cs/Cd Ringer's.

Evaluation of I_{Kx} tail currents. The standard protocol to measure tail currents began with a control recording in 0 Ba^{2+} after a 2.5 min dialysis. Then, successively higher concentrations of Ba^{2+} were superfused with tail currents being obtained after a 3 min superfusion. In deriving conductance-voltage (g–V) curves, tail amplitudes were converted to conductance by dividing the current by the driving force (E–E_r), where E is the tail potential and E_r the reversal potential for I_{Kx}. Conductance-voltage plots were fitted with the Boltzmann equation:

$$g(E) = \frac{g_{max}}{1 + \exp\left(\frac{-(E-E_{1/2})}{S}\right)} \quad (1)$$

where g is conductance, g_{max} the maximal conductance, $E_{1/2}$ the voltage for half-maximal activation, and S the slope factor. The slope factor was converted into equivalent gating charge (Q) by dividing RT/F by the measured slope factor, where the thermodynamic quantity RT/F was 25.5 mV (22°C). Q is an index of the number of charges needed to move all the way across the membrane for channel gating to occur (Hodgkin and Huxley, 1952).

Voltage-dependent block. To model the relative location of Ba^{2+} binding, I assumed that a site at which Ba^{2+} acts is located within the membrane electric field. Assuming Ba^{2+} is

impermeant, a kinetic scheme for this model is (Woodhull, 1973):

$$Ba^{2+} + \text{Site} \underset{k_{off}}{\overset{k_{on}}{\rightleftharpoons}} Ba^{2+}\text{-Site}$$

where k_{on} is the second-order rate constant for binding ($M^{-1}\ s^{-1}$) and k_{off} the first order rate constant for unbinding (s^{-1}). If the site is located within the electric field, both k_{on} and k_{off} will depend on the membrane potential:

$$k_{on}(E) = k_{on}(0) \cdot \exp\left(\frac{-z\delta_{on}E}{RT/F}\right) \tag{2}$$

$$k_{off}(E) = k_{off}(0) \cdot \exp\left(\frac{z\delta_{off}E}{RT/F}\right) \tag{3}$$

and:

$$K_{0.5}(E) = \frac{k_{off}(E)}{k_{on}(E)} = K_{0.5}(0) \cdot \exp\left(\frac{z\delta E}{RT/F}\right) \tag{4}$$

where $k_{on}(0)$ and $k_{off}(0)$ are the voltage-independent rate constants, z the valence of the blocking ion, and $\delta_{on} + \delta_{off} = \delta$; δ is the portion of the membrane electric field sensed by the site. The parameters δ and $K_{0.5}(0)$ were determined by measuring tail current amplitudes in the presence (I_{Ba}) or absence ($I_{control}$) of Ba^{2+}, determining the concentration dependence of $I_{Ba}/I_{control}$ at a constant potential, and plotting $K_{0.5}$ against potential according to the relation:

$$\ln[K_{0.5}(E)] = \ln[K_{0.5}(0)] + \frac{z\delta}{RT/F} \cdot E \tag{5}$$

Kinetic models involving the interaction of channel gating and such voltage-dependent Ba^{2+} ion binding were solved numerically using a first-order Euler integration.

Quantification of 'run-down.' In the absence of Ba^{2+}, tail current amplitudes showed changes with time presumably reflecting cellular dialysis. To quantify these slow changes, g–V curves were measured at the same time points as those used to assess Ba^{2+} actions but with only the Cs/Cd Ringer's being superfused. Compared to the control g–V curve, g_{max} consistently decreased over time, being reduced on average by 31 ± 8% after 15 min. In addition, gating shifted to more negative potentials with $E_{1/2}$ shifted from −41 ± 2 mV to −55 ± 5 mV after 15 min. Q showed little change with time. I characterized these time-dependent conductance and gating changes, often called 'run-down,' by a single exponential decay: the time-corrected $g_{max,corrected} = g_{max}(t)/[1.1 * \exp(-t/\tau)]$ where τ = 43.2 min; and the time-corrected $E_{1/2,corrected} = E_{1/2}(t) + [31.1 - 34.8 * \exp(-t/\tau)]$ where τ = 21.2 min and t is the time after break-in. These factors were used to correct for time-dependent changes in g_{max} and $E_{1/2}$ with the assumption that they occur similarly in Ba^{2+} (see Fig. 3 *B*). They were also used to correct for run-down in the raw tail current amplitudes (I_{tails}); the time-corrected tail currents, $I_{corrected} = I_{tails}(E,t) * g_{corrected}(E)/g(E,t)$ where $g_{corrected}(E)$ is the g-V curve using $g_{max,corrected}$ and $E_{1/2,corrected}$ and $g(E,t)$ the corresponding uncorrected g-V curve.

RESULTS

The aim of these experiments is to quantify how Ba^{2+} interacts with I_{Kx} channels. Some features of I_{Kx} and the basic effect of Ba^{2+} are presented first.

Features of I_{Kx}

I_{Kx} is a time- and voltage-dependent K^+ current that activates between −60 and −30 mV, does not inactivate and has slow gating kinetics (Beech and Barnes, 1989). These features are seen in the 0 Ba^{2+} record of Fig. 1 *A*. At the holding potential of −32 mV, I_{Kx} is almost maximally activated and contributes 45 pA to the 67-pA standing outward current. With negative steps to −52 mV, I_{Kx} deactivates, producing the slow time-dependent decrease in outward current. With positive steps returning to the holding potential, I_{Kx} reactivates, producing slowly developing outward currents, which will be referred to as tail currents.

Gating of I_{Kx} over a broader range of potentials is seen in the 0 Ba^{2+} record of Fig. 2 *A*. At the holding potential, I_{Kx} contributes 53 pA to the 75-pA standing outward

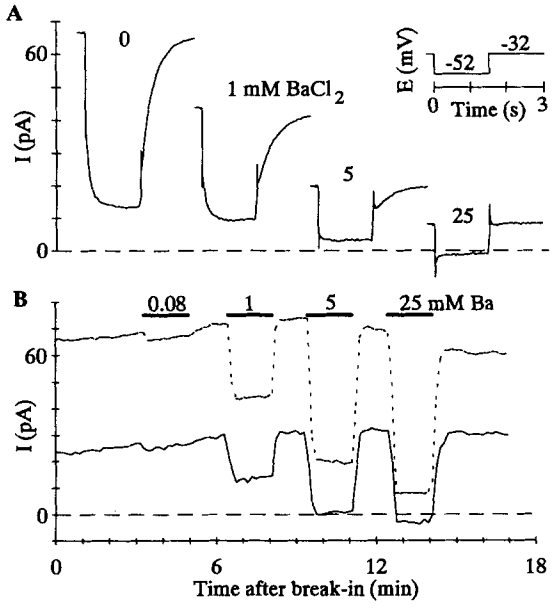

FIGURE 1. Extracellular Ba^{2+} reduces I_{Kx}. (*A*) Whole-cell currents from a rod photoreceptor bathed in Cs/Cd Ringer's with $BaCl_2$ added at concentrations of 0, 1, 5, or 25 mM. Holding potential, −32 mV. (*B*) Amplitude of standing outward current at −32 mV (*dashed line*) and time-dependent current at −52 mV (*solid lines*) for rod in *A* as a function of time after break-in into the whole-cell configuration. Time-dependent currents are the difference between current measured 10–20 ms after the start of the test step and that measured at the end of the same step. Superfusion was continuous and Ba^{2+} was added during times marked by the solid bars.

current. Hyperpolarizing pulses produce a picture closely resembling gating of I_M in sympathetic ganglion cells (Adams et al., 1982*a*). The stronger the hyperpolarization, the faster I_{Kx} deactivates, and between −72 and −82 mV the decaying outward current changes to a decaying inward current, indicating a reversal near the Nernst potential for K^+ (E_K = −88 mV).

Effects of Ba^{2+}

Ba^{2+} is a blocker of many K^+ channels, typically blocking delayed rectifiers and M-currents in the millimolar range, and Ca-activated and inward rectifiers in the micromolar range (Rudy, 1988; Hille, 1992). It also reduces I_{Kx} (Fig. 1). External Ba^{2+} produces a concentration-dependent reduction in I_{Kx} as measured by the loss of

standing outward current at −32 mV (dashed lines) and of the time-dependent current with steps to −52 mV (*solid lines*). This effect is readily reversible on removal of Ba^{2+} from the bathing solution (Fig. 1 *B*).

Fig. 2 *A* contrasts families of whole-cell currents in 0 and 5 mM Ba^{2+}. As in Fig. 1 *A* in 0 Ba^{2+}, I_{Kx} contributes to the standing outward current and shows time- and voltage-dependent gating during and after hyperpolarizing steps. Little further change occurs with small depolarizations, but positive to −2 mV a transient outward current activates which was not further analyzed but appears unrelated to I_{Kx}. In 5 mM Ba^{2+}, currents generated by the same voltage steps are clearly different. The standing outward current at −32 mV is reduced from 75 to 15 pA, and much smaller time-dependent currents are observed during and after hyperpolarizing steps.

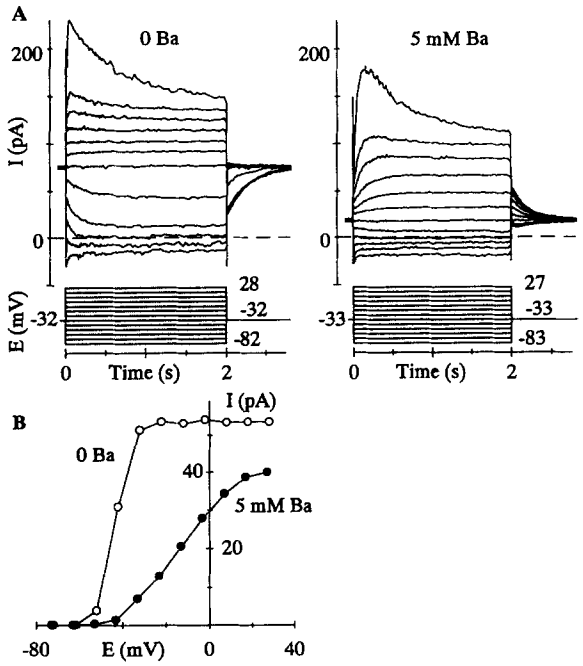

FIGURE 2. In Ba^{2+} time-dependent currents appear at different potentials. (*A*) Families of whole-cell currents in Cs/Cd Ringer's with 0 or 5 mM added Ba^{2+}. (*B*) Peak tail current amplitude from *A*, measured 10–20 ms after the test step, as a function of before test potential.

However, large time-dependent outward currents develop with depolarizing steps, and tail currents at −32 mV are then decaying outward currents. In the absence of Ba^{2+}, the tail-current amplitude reaches a plateau following test steps positive to −32 mV and is steeply voltage dependent between −52 and −32 mV (Fig. 2 *B*). In 5 mM Ba^{2+}, the plateau does not occur until positive to +27 mV, the relationship is less steep, and the peak amplitude is smaller. The transient outward current evoked with positive potential steps in Fig. 2 *A* does not contaminate the tail currents because it is nearly completely inactivated by the end of the 2-s test step.

The nonactivating time-dependent current in 0 Ba^{2+} reflects gating of I_{Kx}. To ask whether the noninactivating time-dependent current in Ba^{2+} is also I_{Kx}, I measured the reversal potential for tail currents and their sensitivity to external TEA. Reversal

potentials were measured with 5 mM external K^+ to make E_K more positive. The tail currents reversed near −66 mV and −64 mV in 0 and 5 mM Ba^{2+}, close to E_K (−70 mV). In 0 Ba^{2+}, 15 mM TEA reduced the tail amplitude at all potentials (to 34 ± 5% of control at −12 mV, n = 3). In Ba^{2+} solutions, the tail currents showed a similar TEA sensitivity: in 5 mM Ba^{2+}, they were reduced to 38% at −13 mV, and in three cells with 1 mM Ba^{2+} they were reduced to 38 ± 3% at −12 mV. The similar reversal potential and TEA sensitivity of tail currents in the absence and presence of Ba^{2+} suggest that the same class of K channels carries the current in the two conditions.

Concentration Dependence of Ba^{2+} Effects on I_{Kx}

As will be shown in the Discussion, the major action of Ba^{2+} probably does not involve a change in the intrinsic gating of I_{Kx} channels but rather a voltage-dependent block. Still, I found it useful to characterize I_{Kx} tail currents in terms of

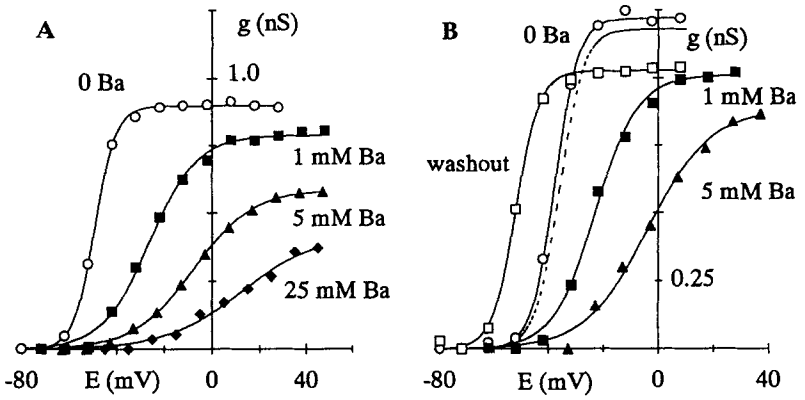

FIGURE 3. Ba^{2+} reduces and shifts I_{Kx} tail current amplitudes. The smooth curves are fitted Boltzmann equations. (*A*) Rod exposed sequentially to 0 (*control*), 1, 5 and 25 mM Ba^{2+}. (*B*) Different rod exposed sequentially to 0, 1, 5, and 0 (*washout*) mM Ba^{2+}. Dashed line is the washout record corrected for 'run-down' (see Materials and Methods).

conductance-voltage (g-V) curves, such as those usually used to describe channel gating, in order to quantify and compare the actions of divalents under different conditions. The I_{Kx} g-V curves for two cells in Fig. 3, *A* and *B*, show that increasing concentrations of Ba^{2+} decreased g_{max}, shifted $E_{1/2}$ in the positive direction, and decreased Q. Fig. 3 *B* also shows a g-V curve obtained after removal of Ba^{2+}. In comparison to the initial control, g_{max} was smaller and $E_{1/2}$ more negative after washout of Ba^{2+}. The dashed line is the washout record corrected for this 'run-down' (see Materials and Methods).

Fig. 4 shows concentration-response curves for the effect of Ba^{2+} on the Boltzmann parameters. Solid circles are uncorrected and the open circles, parameters time-corrected for 'run-down.' Subsequent discussions refer only to the time-corrected parameters. Ba^{2+} produced large concentration-dependent effects on all parameters. However, their concentration dependence differed. To quantify these differences, I

fitted responses with the Hill equation (*dashed lines*):

$$y = \frac{y_{max}}{1 + (K_{0.5}/[Ba^{2+}])^n} \quad (6)$$

where y is the response, y_{max} the maximal response, $K_{0.5}$ the midpoint of the curve and n the Hill coefficient. This transformation is somewhat arbitrary in that it assumes distinct Ba^{2+} binding site(s) and because $E_{1/2}$ does not show complete saturation up to 50 mM Ba^{2+}, but the conclusion obtained from this analysis, that Ba^{2+} has multiple sites of interaction with I_{Kx} channels, is consistent with later results.

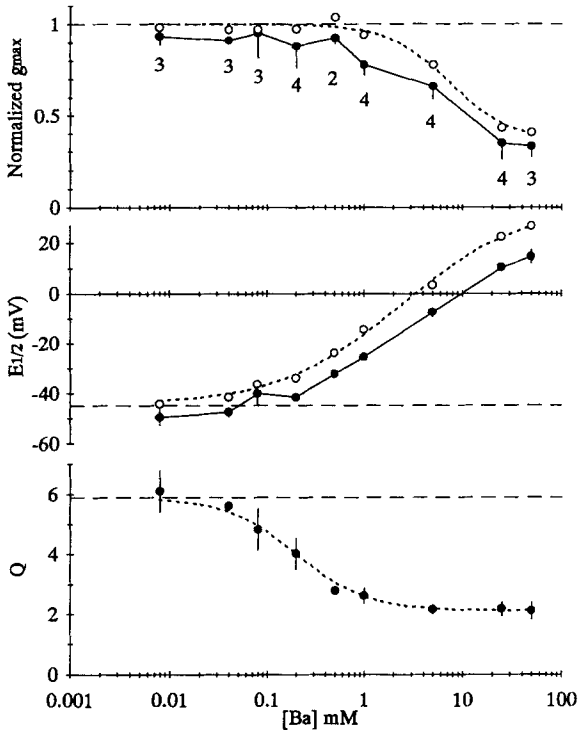

FIGURE 4. Concentration dependence of Ba^{2+} actions. Number of observations made at each concentration shown in g_{max} plot (15 rods). Horizontal dashed lines are control responses measured in 0 Ba^{2+} ~2.5 min after break-in: g_{max}, 1.03 ± 0.04 nS; $E_{1/2}$, −45 ± 1.3 mV; and Q, 5.9 ± 0.1. Solid circles are uncorrected and open circles corrected for time effects. Dashed curves are fitted Hill equations. Some error bars are smaller than the symbols.

Of the three parameters, g_{max} was the least sensitive to Ba^{2+}, being first decreased at 1 mM with a midpoint of 7.6 ± 2 mM, an n of 1.4 ± 0.4 and with a maximal inhibition of 0.65 ± 0.05. In contrast, $E_{1/2}$ and Q were already obviously affected by 0.08 mM, although they had different midpoints: 2.4 ± 0.8 mM for $E_{1/2}$ and 0.2 ± 0.04 mM for Q. The n and y_{max} values were 0.7 ± 0.1 and 80 ± 6 mV for $E_{1/2}$ and 1.3 ± 0.3 and 3.8 ± 0.2 for Q.

Ba^{2+} is Unique in its Effects on I_{Kx} g-V Curves

Barium produced a large shift in $E_{1/2}$. One possible explanation is that Ba^{2+} screens diffuse negative surface charges and hence shifts channel gating (Frankenhauser and Hodgkin, 1957; Gilbert and Ehrenstein, 1969; Hille, Woodhull, and Shapiro, 1975).

For a pure screening hypothesis to be correct, other divalents should produce the same shifts. Fig. 5 shows that Ca^{2+}, Co^{2+}, Mn^{2+}, Sr^{2+}, and Zn^{2+} produced positive shifts in $E_{1/2}$, but in comparison to Ba^{2+} their effects were much smaller. At 25 mM, for example, Zn^{2+} and Co^{2+} shifted $E_{1/2}$ by +21 and +24 mV, respectively, whereas Ba^{2+} shifted it by +65 mV. Also, Co^{2+} shifted $E_{1/2}$ and reduced Q in parallel, but compared to Ba^{2+} both effects were of a much smaller magnitude. Finally, Ca^{2+} and Sr^{2+} produced a reduction in g_{max} similar to that in Ba^{2+}.

In most experiments, 3 mM Ca^{2+} and 0.1 mM Cd^{2+} were included in the Cs/Cd Ringer's. In other experiments, I have found that I_{Kx} g-V curves measured in the absence and presence of 3 mM Ca^{2+} while the rod was exposed continuously to 5 mM

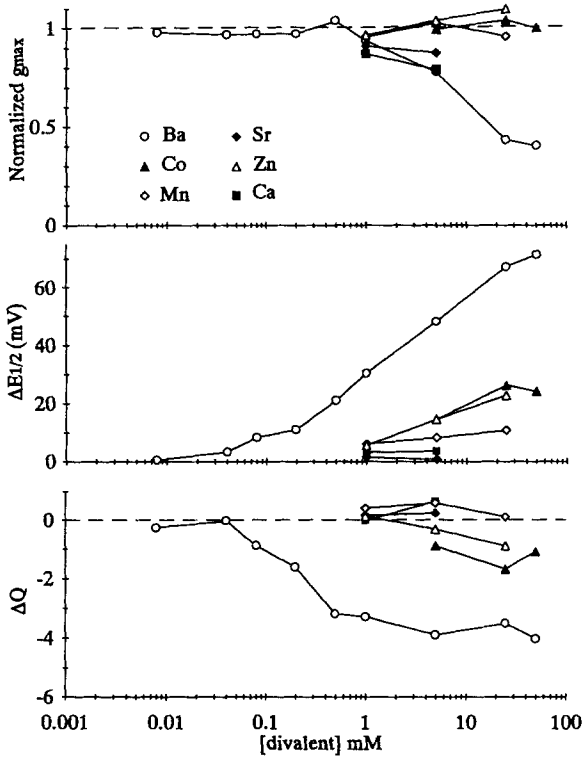

FIGURE 5. Actions of divalent cations on g_{max}, $E_{1/2}$, and Q. Open circles are time-corrected responses in Ba^{2+} from Fig. 4. All points have a minimum of three observations, and g_{max} and $E_{1/2}$ were time-corrected. Values are shown as difference from controls.

Ba^{2+} are essentially identical. Further, previous results have indicated that the I_{Kx} gating is not changed by application of 0.1 mM Cd^{2+} (see Fig. 1 of Beech and Barnes, 1989; cf., Robbins et al., 1992).

High External K^+ Reduces Some Effects of Ba^{2+}

The site(s) at which Ba^{2+} acts may lie within the vestibule or the narrow part of the pore. Because K^+ is the primary permeant ion in I_{Kx} channels and because K^+ and Ba^{2+} have the same crystal radii (0.13 nm), they may compete for similar sites. Therefore, I investigated whether raising external K^+ affects the actions of Ba^{2+}. Initially, however, I had to clarify the effect of very high external K^+ (100 mM) alone.

In 100 mM K^+, E_K is +4 mV and I_{Kx} is now a standing inward current at the holding potential of −32 mV (Fig. 6 *A*). Hyperpolarizing steps deactivate I_{Kx}, producing time-dependent decreases in inward current, and steps back to −42 mV reactivate I_{Kx}, producing increasing inward currents (*tail currents*). High K^+ changed I_{Kx} gating. In Fig. 6 *B*, tail-current *g-V* curves (*solid symbols*) are quite different in 100 and 2.5 mM K^+: g_{max} is nearly three times larger in 100 mM K^+, $E_{1/2}$ is shifted negative to −57 compared with −38 mV, and Q is unchanged (5.9 compared with 5.7). The τ-voltage relation in 100 mM K^+ was also shifted to more negative potentials with the peak near −70 mV; however, the time course at the peak was not greatly different: 260 ± 30 ms (six rods) compared to 290 ± 10 ms in 2.5 mM K^+ (see Fig. 9). In some rods, tail currents at −42 mV could readily be analyzed, but in others, I_{Kx} gating was shifted more negative and tail currents were extremely fast and often contaminated by capacity currents. Hence, in 100 mM K^+, I used the amplitude of the time-dependent current during the voltage step to estimate chord conductance

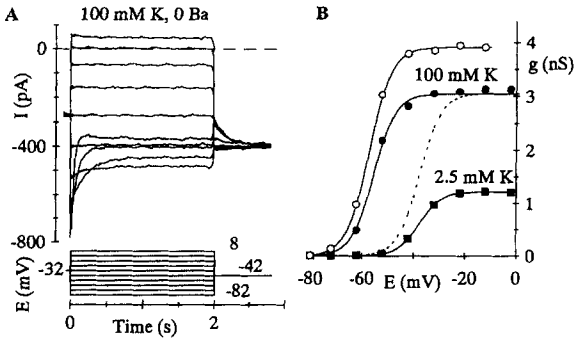

FIGURE 6. High external K^+ shifts the voltage-dependence of I_{Kx}. (*A*) Whole-cell currents in 100 mM K^+, Cs/Cd Ringer's. Positive to −32 mV, I_{Kx} is maximally activated, and currents change from inward to outward near −2 mV (E_{rev} for I_{Kx}). (*B*) Steady-state *g-V* curves derived from tail-current amplitudes (*solid circles*) or chord conductance (*open circles*). Dashed line is 2.5 mM *g-V* curve scaled by 2.55. Chord conductance was determined by dividing the amplitude of the time-dependent current, measured as in Fig. 1, by the driving force for I_{Kx} ($E-E_{rev}$). Capacity currents were subtracted by scaling linear current trace during −22 mV pulse. Smooth curves fitted with Boltzmann equation.

(Fig. 6 *B*, *open circles*). Compared to the tail-current *g-V* curve (*solid circles*), the chord-conductance *g-V* curve had a larger g_{max}, but $E_{1/2}$ and Q were the same. Two other experiments where tail currents were clear enough to measure gave the same pattern.

Adding 5 or 25 mM Ba^{2+} to the 100 K^+ greatly reduced the standing inward current (Fig. 7 *A*). Deactivation of I_{Kx} is seen during hyperpolarizing test steps, and activation, during the steps back to −43 mV (increasing inward tail currents). In Fig. 7 *B* the tail current amplitudes at −43 mV in 25 mM Ba^{2+} are plotted against test voltage (*open circles*). The relationship has two phases with a plateau occurring between −45 and −25 mV. The Boltzmann equation is fitted between −85 and −35 mV, the region that seemed to reflect gating of I_{Kx}. Again, in comparison to this tail current analysis, chord conductance (*solid squares*) gives a slightly higher g_{max} but the same $E_{1/2}$ and Q. Conductance-voltage curves in different Ba^{2+} concentrations (Fig. 7 *C*) show that with increasing Ba^{2+}, g_{max} is progressively reduced but $E_{1/2}$ and Q are hardly changed. Fig. 8 summarizes these results. Changing the external K^+ had no

effect on the Ba^{2+}-induced reduction in g_{max}, whereas increasing K^+ nearly eliminated the effect of Ba^{2+} on $E_{1/2}$ and Q.

Ba^{2+} Changes the Kinetics of I_{Kx} Gating

Some divalent cations change K channel activation and deactivation gating kinetics differentially apparently by binding preferentially to either the open or closed state

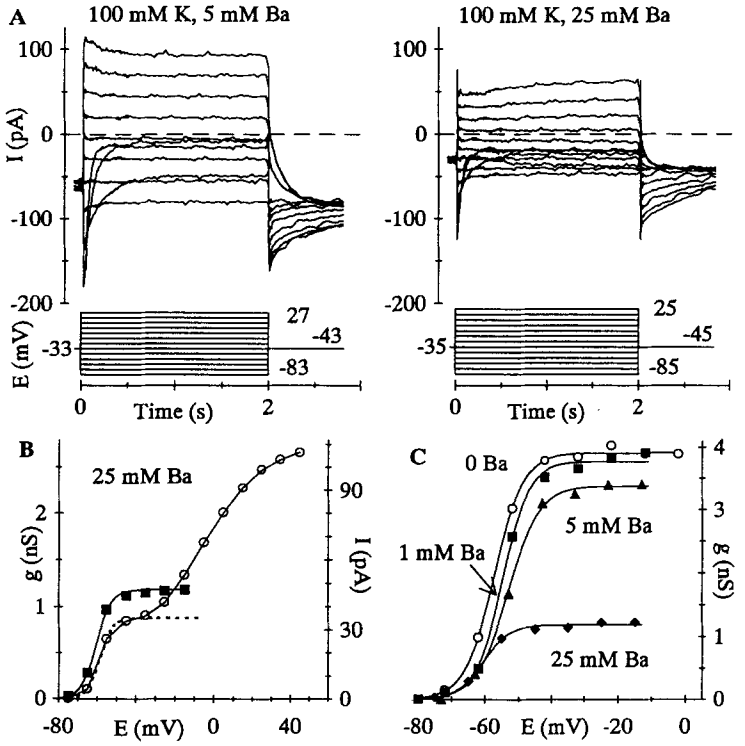

FIGURE 7. Effect of Ba^{2+} on I_{Kx} in 100 mM K^+. (*A*) Whole-cell currents for the rod in Fig. 6 but now with 5 or 25 mM Ba^{2+} added. (*B*) Tail current amplitude (*open circles*) and chord conductance (*solid squares*) for the 25 mM Ba^{2+} record of *A*. Current scale applies to circles. Conductance scale applies to squares and also to circles assuming the tail currents have a E_{rev} the same as that of I_{Kx}. Smooth curve through the squares and dashed line through the first five circles (−85 to −35 mV) are fitted Boltzmann equations. (*C*) Chord-conductance *g-V* curves for the rod in Figs. 6 *A* and 7 *A* exposed sequentially to 0, 1, 5, and 25 mM Ba^{2+}.

(e.g., Gilly and Armstrong, 1982). In 0 Ba^{2+}, the time courses of I_{Kx} deactivation and activation were similar and were well described by a single exponential (see also Beech and Barnes, 1989). The combined deactivation and activation time constants in 0 Ba^{2+} are shown as open squares in Fig. 9 *B*. In general, the time course of I_{Kx} in Ba^{2+} was also well described by single exponentials. However, in 0.2 mM Ba^{2+}, the fits sometimes missed many of the points and could often but not always be improved by using two exponentials; the points in Fig. 9 *A* include only those responses well

described by a single exponential. In 0.2 mM Ba^{2+}, apparent deactivation and activation time constants could both be measured only between −42 and −22 mV, but in this voltage range they were obviously unequal (Fig. 9 *A*). In addition, the time constants at the peak of the τ-voltage relations are slower than those in 0 Ba^{2+}. In contrast, in higher Ba^{2+} concentrations, apparent deactivation and activation time courses were equally affected. Also, relative to 0.2 mM Ba^{2+}, the time constants in higher Ba^{2+} are speeded up and shifted to more positive potentials and the voltage dependence is reduced. Finally, in 5 and 25 mM Ba^{2+} (Figs. 9, *C* and *D*), the slowest time constants occurring at the peak of the τ-voltage relation are faster than those in 0 Ba^{2+}. Thus the effects of Ba^{2+} on I_{Kx} kinetics are complex and concentration-

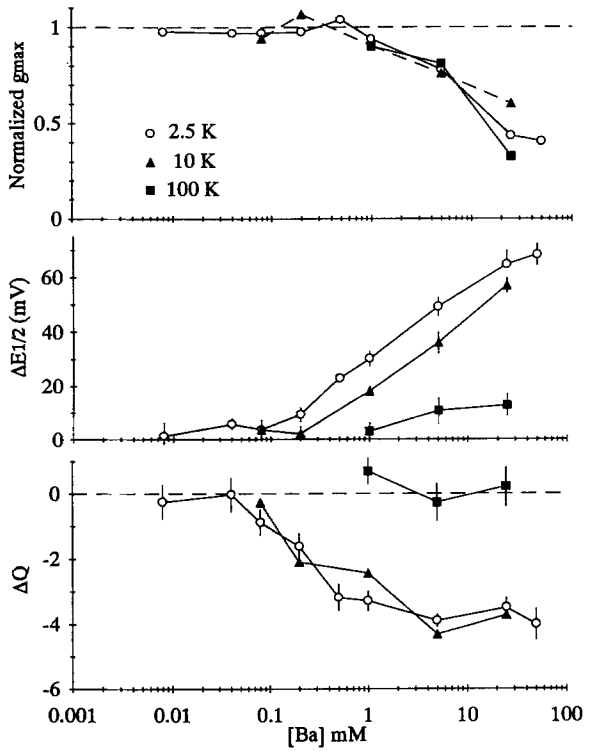

FIGURE 8. Action of Ba^{2+} on $E_{1/2}$ and Q but not g_{max} is reduced by high external K^+. The 2.5 mM K^+ plots are from Fig. 5. For 10 mM K^+, *g-V* curves derived from tail currents (eight rods), and control values: g_{max}, 1.2 ± 0.1 nS; $E_{1/2}$, −43 ± 1 mV; and Q, 6.6 ± 0.3. For 100 mM K^+, *g-V* curves derived from chord conductance (six rods), and control values: g_{max}, 5.4 ± 0.5 nS; $E_{1/2}$, −70 ± 4 mV; and Q, 6.7 ± 0.3. All g_{max} and $E_{1/2}$ responses are corrected for run-down. Each point has a minimum of 3 (10 mM K^+) or 4 (100 mM K^+) observations.

dependent. A model which can reproduce some of these effects of Ba^{2+} is presented in the Discussion.

Concentration Jumps of Ba^{2+}

In squid axons, where Ba^{2+} enters K channels to block them, the rate at which block appears with millimolar Ba^{2+} is much slower than the rate of channel gating (Armstrong and Taylor, 1980; Armstrong, Swenson, and Taylor, 1982). To test the rate at which Ba^{2+} interacts with I_{Kx} channels, I applied Ba^{2+} rapidly. In an initial calibration run, the exchange of K^+ ions (20 mM) was found to develop with an exponential time constant τ = 17 ± 3 ms (n = 4). Rapid perfusion of 5 mM Ba^{2+}

decreased the standing outward current with a time constant τ = 180 ms (Fig. 10 *A*). Interestingly, the rate of decrease of I_{Kx} during rapid application of 5 mM Ba^{2+} at −33 mV is indistinguishable from the apparent time course of I_{Kx} deactivation measured with steady 5 mM Ba^{2+} during a voltage step to −33 mV (Figs. 10, *A* and *B*). Such similarity in the rate of action of Ba^{2+} and the rate of gating in Ba^{2+} solutions was observed at membrane potentials between −22 and −47 mV (Fig. 10 *C*).

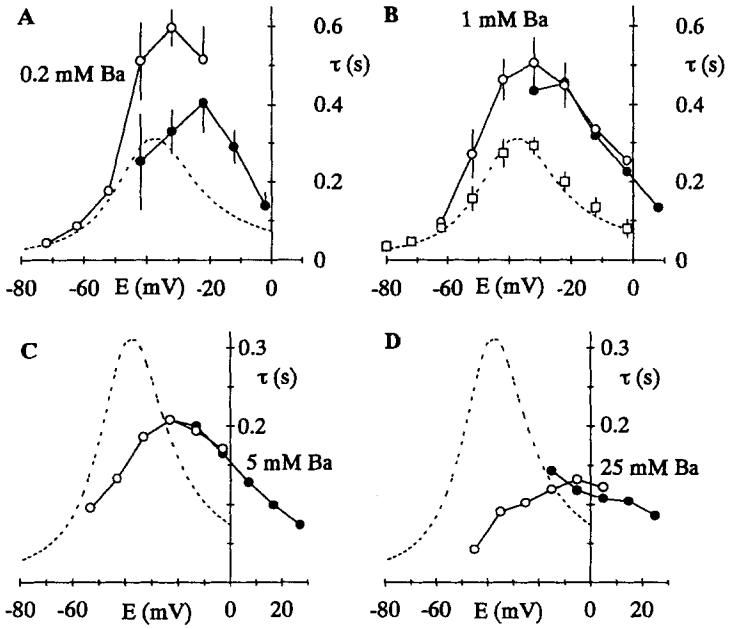

FIGURE 9. Concentration dependent effects of Ba^{2+} on I_{Kx} kinetics. Average exponential time constants (τ) for activation (*solid circles*) or deactivation (*open circles*) plotted against test potential. In *B*, open squares are τ's obtained in 0 Ba^{2+} (eight rods) with activation and deactivation responses combined. Dashed curve is $1/(\alpha + \beta)$, where α and β are rate constants for transitions between closed and opened states of the channels. Mean values for α and β were calculated from $\alpha = A_{ss}/\tau$ and $\beta = (1 - A_{ss})/\tau$ (Hodgkin and Huxley, 1952), where A_{ss} is the normalized steady-state conductance, and τ is the time constant of the fitted exponential. α and β were fitted by eye with the functions: $\alpha = 0.36(E + 33)/(1 - \exp(-(E + 33)/6.9))$; $\beta = 1.34(E + 58.5)/(\exp[E + 58.5]/6.9 - 1)$, where E is the membrane potential (mV). The curve $1/(\alpha + \beta)$ is redrawn in all plots. (A) 0.2 mM Ba^{2+}, six rods. (*B*) 1 mM Ba^{2+}, five rods. (*C*) 5 mM Ba^{2+}, seven rods. (*D*) 25 mM Ba^{2+}, four rods. Near the peak of each curve, except 25 mM, a minimum of five observations were made for each potential. Error bars shown only for selected responses.

One interpretation of these results is that the 180 ms time constant reflects the time course of a slow block of I_{Kx} channels by Ba^{2+}. Alternatively, Ba^{2+} may interact with I_{Kx} channels more quickly yielding a Ba^{2+} modified channel with new gating characteristics (e.g., an allosteric action). In this case, application of Ba^{2+} before a voltage step should quickly generate Ba^{2+}-modified channels with gating characteris-

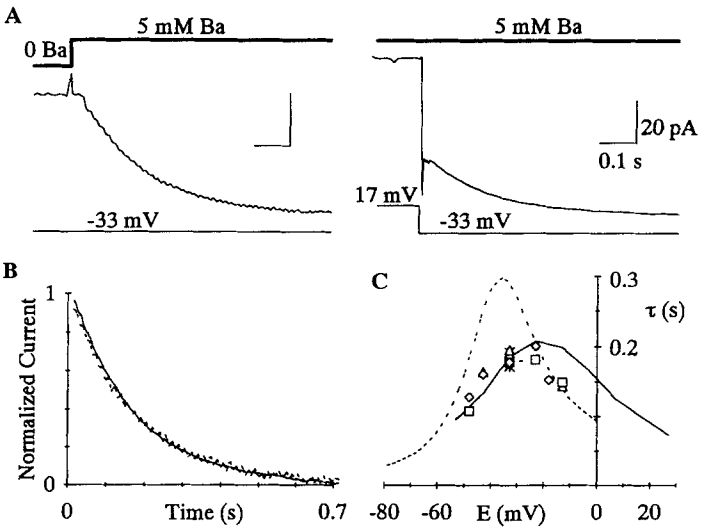

FIGURE 10. Concentration jump experiments. (*A*) Currents resulting from a concentration jump of 5 mM Ba^+ at a constant voltage, −33 mV (*left*) and from a voltage step from +17 mV to −33 mV in the presence of constant 5 mM Ba^{2+} (*right*). (*B*) Comparison of time-dependent currents in (*A*) for concentration jump (*dashed line*) and voltage step (*solid line*). Time zero refers to time of onset of the fitted exponential. Currents are normalized: = $(R - R_{min})/(R_{max} - R_{min})$ where R is the current at a given time and R_{min} and R_{max} the minimum and maximum currents. (*C*) Comparison of current kinetics in response to concentration jumps of 5 mM Ba^{2+} (*symbols*) with voltage-activated I_{Kx} kinetics in 0 Ba^{2+} ($1/(\alpha + \beta)$, *dashed line*) or 5 mM Ba^{2+} (mean values joined by continuous line) (from Fig. 9). Different symbols are responses from different rods.

tics like those in continuous Ba^{2+}. Fig. 11 illustrates the rapid wash-on of 5 mM Ba^{2+} just before a voltage step. Compared to the currents following the same voltage step but in constant 0 or 5 mM Ba^{2+}, the tail currents following rapid application of Ba^{2+} are mixed, initially getting increasingly outward but then slowly changing to decreasingly outward and only near the end of the voltage step approaching the tail currents in constant 5 mM Ba^{2+}. This mixed current response is not a result of the slow arrival

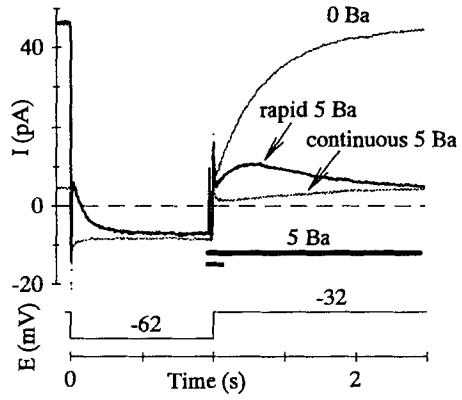

FIGURE 11. The rate of action of Ba^{2+} is slow. Three overlapped whole-cell current traces during a voltage step for a rod exposed continuously to 0 or 5 mM Ba^{2+} (*thin traces*) or a concentration jump from 0 to 5 mM Ba^{2+} near the end of the step to −62 mV (*thick trace*). The shaded bar indicates the time required for rapid application of 20 mM K^+, under identical conditions, to reach steady-state (total time 125 ms).

of Ba^{2+} because the Ba^{2+} concentration has presumably reached steady-state by the end of the shaded period. As will be argued in the Discussion, this mixed current time course argues against rapid Ba^{2+} binding and suggests that the time course of currents with rapid application of Ba^{2+} or in constant Ba^{2+} reflects the slow kinetics of the action of Ba^{2+}.

Voltage-Dependent Block by Ba^{2+}

If the time dependence of currents in the presence of Ba^{2+} does reflect the slow block and unblock of I_{Kx} channels by Ba^{2+}, peak tail currents will be an index of the relative number of blocked channels during the prior voltage step. Fig. 12 *A* shows the relative tail current amplitude, $I_{Ba}/I_{control}$, at two potentials, while Fig. 12 *B* shows

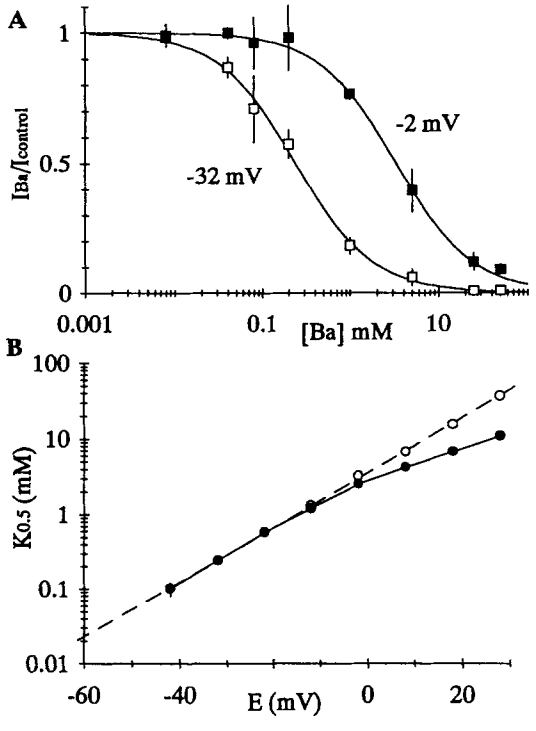

FIGURE 12. Voltage-dependent block of I_{Kx} by Ba^{2+}. (*A*) Relative tail current amplitude in the presence (I_{Ba}) or absence ($I_{control}$) of Ba^{2+} after test steps to either −32 mV (*open squares*) or −2 mV (*closed squares*). Tail currents were corrected for 'run-down' (see Materials and Methods) and for a voltage-independent bocking action of Ba^{2+} (see Results). Smooth curves are fitted Hill equations with $K_{0.5}$s of 0.24 mM (−32 mV) and 3.3 mM (−2 mV). Records are from the same tail currents as those used to derive *g-V* curves in Fig. 5 (15 rods). (*B*) $K_{0.5}$ as a function of the test potential. $K_{0.5}$ are derived from fits to tail currents which were uncorrected (*closed circles*) or corrected (*open circles*) for a voltage-independent blocking action. All fits to subtracted responses had Hill coefficients between 0.9–1.1 (±0.1) whereas for unsubtracted responses, at potentials positive to −2 mV, the Hill coefficient ≥ 1.3.

$K_{0.5}$s derived from Hill equation fits of $I_{Ba}/I_{control}$ over the range of potentials where I_{Kx} tail currents could be reliably measured or where $I_{control}$ was not too small. The points in Fig. 12 *A* and the open circles in Fig. 12 *B* are derived from tail currents after correction for an assumed voltage-independent blocking action of Ba^{2+} (*dashed curve* in the g_{max} plot in Fig. 4). This assumption of a voltage-independent component of action seems justified since strong depolarizations did not relieve the reduction in g_{max}. The $K_{0.5}$s derived from corrected tails in Fig. 12 *B* is described by Eq. 5 with parameters of δ, 1.07 ± 0.02 and $K_{0.5}(0)$, 3.6 ± 1 mM.

DISCUSSION

For I_{Kx} channels, Ba^{2+} stands out among the divalent ions tested in the range and strength of its effects. However, not all of its actions need be closely related. The depression of g_{max} by Ba^{2+} seems to be separable from the shift in $E_{1/2}$ and the change in Q. Unlike the other two actions, the depression of g_{max} begins only at high Ba^{2+} concentrations ($K_{0.5}$ = 7.6 mM), is not reversed by raising external K^+, and was nonspecific because Ca^{2+} and Sr^{2+} had similar actions (cf, Robbins et al., 1992). The depression of g_{max} by Ba^{2+} also appears to occur in a voltage-independent manner since it was not relieved by depolarization. On the other hand, the Ba^{2+}-induced shift in $E_{1/2}$ and the change in Q first appeared at a low concentration and were highly K^+ sensitive. There is no clear indication whether these two effects have a common origin. An argument for two separate sites is the higher sensitivity of the change in Q ($K_{0.5}$ = 0.2 mM) versus the shift in $E_{1/2}$ ($K_{0.5}$ = 2.4 mM). However, if part of the shift is due to another mechanism, such as shielding of negative surface charges, removing this action would shift the concentration-response curve for $E_{1/2}$ leftward, reducing the disparity in the concentration dependence of $E_{1/2}$ and Q. Indeed, as is shown below, both of these actions can be ascribed to the same mechanism, a steeply voltage-dependent blocking action by Ba^{2+} that is kinetically slow. However, before addressing this blocking model, I will consider three other hypothesis that might account for the shift in $E_{1/2}$: (*a*) Ba^{2+} shields fixed negative surface charges; (*b*) Ba^{2+} stabilizes either the closed or open state of the channel; and (*c*) Ba^{2+} acts on an allosteric site.

Cations can shield fixed negative charges on the channel by creating a diffuse double layer and changing the local potential seen by the voltage sensor (Frankenhauser and Hodgkin, 1957; see Hille, 1992). For external cations this would bias positively the voltage dependence of channel gating (hypothesis *a*). A pure shielding mechanism cannot account for the large Ba^{2+}-induced shift. First, Ba^{2+} was almost two orders of magnitude more potent in producing shifts of I_{Kx} than Ca^{2+}, Co^{2+}, Mn^{2+}, Sr^{2+} and Zn^{2+} (cf, Mozhayeva and Naumov, 1972; Hille et al., 1975; Cukierman, Zinkind, French, and Krueger, 1988). Second, in a shielding mechanism, ions are concentrated at the surface because of a local potential from the surface charge, and the partition of ions between the bulk solution and the charged surface depends only on their valence but not on their chemical nature. Hence, changing the monovalent ion from Na^+ to K^+ should not reduce the effects of the divalent Ba^{2+}, yet replacing external Na^+ with K^+, greatly reduced the Ba^{2+}-induced shift of $E_{1/2}$. Hence, Ba^{2+} apparently interacts with I_{Kx} channels at a site where other physical properties, such as ionic radius or dehydration energy, are important.

Although a simple shielding mechanism cannot account for the large Ba^{2+}-induced shift in $E_{1/2}$, it may contribute to this action. Indeed, the K^+-insensitive component of the Ba^{2+}-induced shift (Fig. 8) is also on the same order of magnitude as that produced by other divalents. A shielding mechanism would also account for the lack of saturation in the shift at high Ba^{2+} concentrations (Fig. 4).

Some divalents differentially alter the activation or deactivation time course of delayed rectifier K channels, apparently by stabilizing either the closed- or the open-state (hypothesis *b*) (Begenisich, 1988). For example, Ba^{2+} and Ca^{2+} slow the

time course of activation but not deactivation of I_K in squid axon, presumably by stabilizing the closed-state (Armstrong et al., 1982; Armstrong and Matteson, 1986; Armstrong and Lopez-Barneo, 1987; Armstrong and Miller, 1990; see also Miller, 1987, Grissmer and Cahalan, 1989). Gilly and Armstrong (1982) interpreted a Zn-induced slowing of I_K activation but not deactivation as reflecting a direct binding of Zn^{2+} to the gating charges in the closed state. Indeed, for I_{Kx} channels, Zn^{2+} also greatly slowed the time course for activation relative to that for deactivation (Wollmuth, unpublished observations). However, Ba^{2+}, at concentrations higher than 0.2 mM, does not appear to stabilize either the open- or closed-state preferentially. For example, in 1 mM Ba^{2+} both activation and deactivation were slowed relative to the control, and at potentials where both parameters could be measured, they were essentially identical. Also, the slowing of deactivation relative to activation at 0.2 mM Ba^{2+}, if interpreted as a stabilization of the open state, would predict a negative shift of the voltage dependence of gating, contrary to the observed positive shift.

The similarity in the rate of action of Ba^{2+} and the apparent rate of gating in Ba^{2+} solutions (Fig. 10) could either mean that Ba^{2+} is plugging I_{Kx} channels at this rate (see blocking model) or alternatively, that it reaches a modulatory binding site quickly but yields a Ba^{2+}-modified I_{Kx} with new gating characteristics (hypothesis *c*). However, if Ba^{2+} is binding rapidly to a modulatory site, than in Fig. 11 when the concentration of Ba^{2+} reaches steady-state, all I_{Kx} channels would be in this Ba^{2+}-modified mode and the overall tail current would have a time course approaching that in continuous 5 mM Ba^{2+}. In contrast, what is observed is a mixed current response occurring long after the Ba^{2+} solution change reached steady state, which presumably reflects channels going slowly from the closed to opened states and from closed/opened to blocked states.[1] Although these results do not directly rule out an allosteric model, they strongly suggest that the kinetics of action of intermediate concentrations of Ba^{2+} are similar to the time course of I_{Kx} gating. The most likely explanation is that the time dependence of currents in Ba^{2+} reflect the voltage-dependent binding and unbinding of Ba^{2+} in a blocking process.

Blocking model. Voltage-dependent block has been used to describe the actions of Ba^{2+} on many K channels, including inward rectifiers (Hagiwara et al., 1978), delayed rectifiers (Armstrong et al., 1982), Ca-activated K channels (Vergara and Latorre, 1983; Miller, Latorre, and Reisin, 1987) and M-like currents in neuroblastoma cells (Robbins et al., 1992). For my data, the putative voltage-dependent block by Ba^{2+} was quantified by assuming that the process causing depression of g_{max} is not voltage-dependent (see also Robbins et al., 1992). The remaining action of Ba^{2+} was found to be steeply voltage-dependent with an apparent electrical distance (δ) of 1.07. Because δ is greater than unity, it probably reflects the combined electrical distances of Ba^{2+} and one or more K^+ ions entering the pore in a multi-ion process (Hille, 1992). However, a unique interpretation cannot be assigned to δ (Armstrong et al., 1982). Hence, a δ of 1.07 could reflect that in going from the unblocked to blocked state one Ba^{2+} traverses the membrane completely while two K^+ ions go 7%

[1] It should be noted that the results in Fig. 11 do not address whether Ba^{2+} can block closed and open channels or only open channels since either blocking reaction is consistent with the observed current.

across or alternatively, it may reflect that one Ba^{2+} goes 50% across while two K^+ ions go 57% across.

Ba^{2+} and K^+ have the same crystal radius, and Ba^{2+} can substitute for K^+ in the permeation pathway in some K channels (Neyton and Miller, 1988*a*, *b*). Consistent with the voltage-dependent action of Ba^{2+} being in the permeation pathway is the reduction by K^+ of the Ba^{2+}-induced shift in $E_{1/2}$ and change in Q (see below). Little is known about the permeation pathway of M-like channels, but my results suggest that as in other K channels, Ba^{2+} can bind within the permeation pathway and that I_{Kx} channels have multi-ion pores (Hille, 1992).

To explore voltage-dependent blocking mechanisms, I modeled I_{Kx} currents in the presence of Ba^{2+}, testing two different voltage-dependent blocking schemes. In Scheme I Ba^{2+} acts as an open-channel blocker and must wait for the channel to open before it can bind:

$$C \underset{\beta}{\overset{\alpha}{\rightleftharpoons}} O + Ba^{2+} \underset{k_{off}}{\overset{k_{on}}{\rightleftharpoons}} O\text{-}Ba^{2+}$$

SCHEME I

In Scheme 2 Ba^{2+} can bind to I_{Kx} channels in either the closed or open state:

$$\begin{array}{ccc} C & \underset{\beta}{\overset{\alpha}{\rightleftharpoons}} & O \\ k_{on} \downarrow\uparrow k_{off} & & k_{on}' \downarrow\uparrow k_{off}' \\ C\text{-}Ba^{2+} & \underset{\beta'}{\overset{\alpha'}{\rightleftharpoons}} & O\text{-}Ba^{2+} \end{array}$$

SCHEME II

where α and β are rate constants for transitions between closed (C) and opened (O) states of the channel (equations describing α and β are found in the legend of Fig. 9), and k_{on} and k_{off} are the voltage-dependent rate constants for Ba^{2+} binding and unbinding (Eqs. 2 and 3). In Scheme II the simplifying assumption is made that $\alpha = \alpha'$, $\beta = \beta'$, $k_{on} = k'_{on}$, and $k_{off} = k'_{off}$. Because δ (= 1.07) and $K_{0.5}(0)$ (= 3.6 mM) could be measured (Fig. 12), only two free parameters remained: either δ_{on} or δ_{off} and $k_{on}(0)$ or $k_{off}(0)$. In the following analysis I varied δ_{on} and $k_{on}(0)$ systematically.

Several conclusions emerged: The steady-state currents calculated from either scheme are identical regardless of which δ_{on} and $k_{on}(0)$ were selected (e.g., Fig. 13). Therefore, predicted steady-state tail current amplitudes cannot distinguish between schemes or the appropriateness of either δ_{on} or $k_{on}(0)$ values. To distinguish between schemes required examining the time-course of predicted currents. On this basis, Scheme I had to be rejected since it showed current time courses never observed. In particular, when $k_{on}(0)$ was given values $\leq 5{,}000$ M^{-1} s^{-1}, the apparent activation time course of currents at potentials > -20 mV showed two distinct kinetic components reflecting the rapid opening of I_{Kx} channels and then the slow block by Ba^{2+} (e.g., Fig. 13), and when $k_{on}(0)$ was given values $> 5{,}000$ M^{-1} s^{-1}, currents

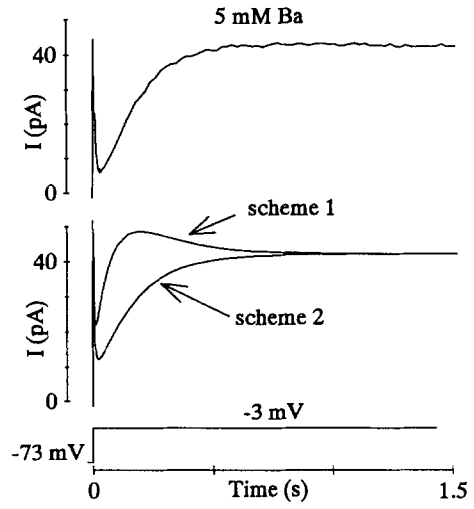

FIGURE 13. Comparison of model I_{Kx} currents with recorded currents in 5 mM Ba^{2+}. Model currents were generated using either Scheme 1 or 2 with k_{on} (0) = 700 M^{-1} s^{-1} and δ_{on} = 0.15 and include a small leak conductance that is insensitive to Ba^{2+} (G_{leak}/G_{Kx} = 0.2; E_{leak} = −54 mV; E_{Kx} = −75 mV). Transient currents occurring during the voltage step in 0 Ba^{2+} are included in the model currents.

during deactivation showed mixed kinetic components: with steps to negative potentials, open channels rapidly became blocked by Ba^{2+} and then, very slowly, became unblocked and entered into the closed state. On the other hand, Scheme II with $k_{on}(0)$ at 700 M^{-1} s^{-1} and δ_{on} = 0.15 replicated many aspects of the actions of Ba^{2+}. The parameters, $k_{on}(0)$ and δ_{on}, were selected to fit the apparent activation and deactivation time course of recorded currents in 5 mM Ba^{2+}. Fig. 14 *A* shows model currents in 0 Ba^{2+} and in 5 mM Ba^{2+}, which are quite similar to recorded currents in Fig. 2. Fig. 14 *B* shows predicted tail current amplitudes and contrasts them with the

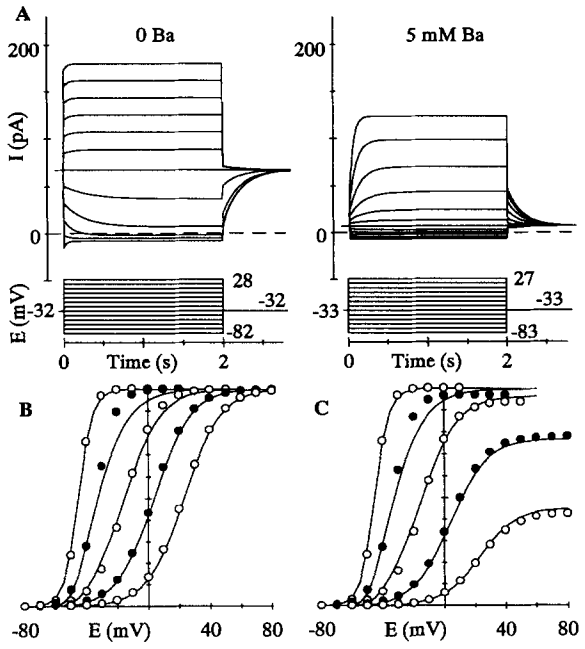

FIGURE 14. Model I_{Kx} currents. (*A*) Families of model currents in 0 Ba^{2+} or in 5 mM Ba^{2+} using Scheme 2 with k_{on} (0) = 700 M^{-1} s^{-1} and δ_{on} = 0.15. Currents include a voltage-independent blocking action of Ba^{2+} (see Fig. 12) and a small leak conductance (see Fig. 13). (*B*) Steady-state tail current amplitudes assuming only a voltage-dependent blocking mechanism for model currents (*solid lines*) and averages *g-V* curves from left to right, 0, 0.2, 1, 5, 25 mM Ba^{2+}. All responses are set to unity. (*C*) Same as in *B* but now including the voltage-independent blocking action.

average g-V curves measured in Ba^{2+}. At least for 1, 5, and 25 mM Ba^{2+}, the voltage-dependent action of Ba^{2+} can account for the shift in $E_{1/2}$ and change in Q. Fig. 14 *C* includes the voltage-independent blocking action of Ba^{2+} which was described by a Hill equation (see Fig. 12) and which depresses the maximal current.

The simple blocking model (Scheme II) reproduced many features of the action of Ba^{2+}. Nevertheless, some discrepancies remain. First, while the time courses of modeled currents for 5 mM Ba^{2+} were essentially identical to measured currents, for 1 and 25 mM Ba^{2+}, they showed a quantitative difference. The time course of model currents for 1 mM Ba^{2+} were slower whereas those for 25 mM Ba^{2+} were faster than those recorded. (Also, at negative potentials in the model, the time course of apparent activation currents was slower than that of apparent deactivation; however, this deviation occurred only at potentials where empirically only deactivation could be measured.) Second, the model did not reproduce the actions of low concentrations (0.2 mM) of Ba^{2+} on steady-state tail currents (Fig. 14 *B*) or on the apparent activation and deactivation time course (Fig. 9 *A*). These discrepencies probably reflect that the assumptions of Scheme II need to be refined further and that there may be more subtle actions of Ba^{2+} on I_{Kx} channels. Nevertheless, Scheme II appears to encompass the basic elements of the major action of Ba^{2+} on I_{Kx} channels.

In my experiments, high K^+ prevented most of the Ba^{2+}-induced shift in $E_{1/2}$ and change in Q. If one simply assumes a competitive action between the voltage-dependent action of Ba^{2+} and K^+, then the model can generate the currents during test steps and the rapid tail currents following steps to negative potentials. However, there are also slowly decaying tail currents seen following steps to depolarized potentials (Fig. 7 *A*). These decaying tails not present in 0 Ba^{2+} (Fig. 6 *A*), could reflect reentry of Ba^{2+} ions, kicked out during the depolarized test step, but the model in its simplest form cannot account for these tails. Alternatively, two lines of evidence suggest that these slowly decaying tails may be unrelated to the action of Ba^{2+} on I_{Kx}. First, the total tail current amplitude in 1 or 5 mM Ba^{2+} is greater than that in 0 Ba^{2+}, suggesting that additional current is being generated in 100 mM K^+, $BaCl_2$. Second, the time course of decay is not appreciably dependent on the $BaCl_2$ concentration, if anything being slower at higher concentrations (cf, Fig. 9).

Effect of high K^+ on I_{Kx}. High K^+ induced a negative shift in the voltage range of activation and increased macroscopic conductance for I_{Kx} gating (Fig. 6 *B*). The negative shift in the voltage dependence in high K^+ has been observed for other K channels, including delayed rectifiers (e.g., Swenson and Armstrong, 1981; Matteson and Swenson, 1986). Because I_K deactivation, but not activation, was slowed in these previous studies, occupancy of the permeation pathway by K^+ was assumed to antagonize channel closing ('foot-in-the-door hypothesis'), shifting the voltage dependence negative. In contrast, for I_{Kx} channels in high K^+, the τ-voltage relation was simply shifted leftward with no differential effect on deactivation or activation kinetics. Therefore, the mechanism by which K^+ affects gating of I_{Kx} channels may be different from that in other K channels.

Relation to M-current. The action of divalents on M-like currents is not uniform. Like I_{Kx} channels, the channels underlying $I_{K(M,ng)}$, an M-like current described in neuroblastoma cells (Robbins et al., 1992), appear to be blocked in a voltage-dependent and voltage-independent manner by Ba^{2+}. On the other hand, Ba^{2+}

appears to block I_M channels in sympathetic ganglion cells apparently only in a voltage-independent manner (Beech and Barnes, 1989; Robbins et al., 1992). In addition, there appear to be differences between I_{Kx} and $I_{K(M,ng)}$ in terms of block by divalents such as Zn^{2+} (Robbins et al., 1992). These differences suggest that at the molecular level there is a family of M-like channels of which I_{Kx} is a member, but that M-like channels vary in their permeation pathways.

I thank Dr. Bertil Hille for his assistance and in whose laboratory all of the work was performed, Dr. D. Beech for help with the rapid application experiments and insightful discussions, Drs. M. S. Shapiro, J. Herrington and A. P. Naumov for their comments on the manuscript, Lea Miller for secretarial assistance, and Don Anderson for technical assistance.

This work was supported by a National Institute of Health research grant, NS-08174 and a Research Award from the McKnight Endowment for the Neurosciences to Dr. Bertil Hille, and a NIH Training Grant GM-07108 (L. P. Wollmuth).

Original version received 21 May 1993 and accepted version received 14 September 1993.

REFERENCES

Adams, P. R., D. A. Brown, and A. Constanti. 1982*a*. M-currents and other potassium currents in bullfrog sympathetic neurones. *Journal of Physiology.* 330:537–572.

Adams, P. R., D. A. Brown, and A. Constanti. 1982*b*. Pharmacological inhibition of the M-current. *Journal of Physiology.* 332:223–262.

Armstrong, C. M., and J. Lopez-Barneo. 1987. External calcium ions are required for potassium channel gating in squid axons. *Science.* 236:712–714.

Armstrong, C. M., and D. R. Matteson. 1986. The role of calcium ions in the closing of K channels. *Journal of General Physiology.* 87:817–832.

Armstrong, C. M., and C. Miller. 1990. Do voltage-dependent K^+ channels require Ca^{2+}? A critical test employing a heterologous expression system. *Proceedings National Academy of Sciences, USA.* 87:7579–7582.

Armstrong, C. M., R. P. Swenson, Jr., and S. R. Taylor. 1982. Block of squid axon K channels by internally and externally applied barium ions. *Journal of General Physiology.* 80:663–682.

Armstrong, C. M., and S. R. Taylor. 1980. Interaction of barium ions with potassium channels in squid giant axons. *Biophysical Journal.* 30:473–488.

Attwell, D., and M. Wilson. 1980. Behaviour of the rod network in the tiger salamander retina mediated by membrane properties of individual rods. *Journal of Physiology.* 309:287–315.

Beech, D. J., and S. Barnes. 1989. Characterization of a voltage-gated K^+ channel that accelerates the rod response to dim light. *Neuron.* 3:573–581.

Begenisich, T. 1988. The role of divalent cations in potassium channels. *Trends in Neuroscience.* 11:270–273.

Bernheim, L., D. J. Beech, and B. Hille. 1991. A diffusible second messenger mediates one of the pathways coupling receptors to calcium channels in rat sympathetic neurons. *Neuron.* 6:859–867.

Cukierman, S., W. C. Zinkand, R. J. French, and B. K. Krueger. 1988. Effects of membrane surface charge and calcium on the gating of rat brain sodium channels in planar bilayers. *Journal of General Physiology.* 92:431–447.

Eaton, D. C., and M. S. Brodwick. 1980. Effects of barium on the potassium conductance of squid axon. *Journal of General Physiology.* 75:727–750.

Frankenhaeuser, B., and A. L. Hodgkin. 1957. The action of calcium on the electrical properties of squid axons. *Journal of Physiology.* 137:218–244.

Gilbert, D. L., and G. Ehrenstein. 1969. Effect of divalent cations on potassium conductance of squid axons: determination of surface charge. *Biophysical Journal.* 9:447–463.

Gilly, W. F., and C. M. Armstrong. 1982. Divalent cations and the activation kinetics of potassium channels in squid giant axons. *Journal of General Physiology.* 79:965–996.

Grissmer, S., and M. D. Cahalan. 1989. Divalent ion trapping inside potassium channels of human T lymphocytes. *Journal of General Physiology.* 93:609–630.

Hamill, O. P., A. Marty, E. Neher, B. Sakmann, and F. J. Sigworth. 1981. Improved patch-clamp techniques for high-resolution current recording from cells and cell-free membrane patches. *Pflügers Archiv.* 391:85–100.

Hagiwara, S., S. Miyazaki, W. Moody, and J. Patlack. 1978. Blocking effects of barium and hydrogen ions on the potassium current during anomalous rectification in the starfish egg. *Journal of Physiology.* 279:167–185.

Hille, B. 1992. Ionic Channels of Excitable Membranes. Sinauer Associates Inc., Sunderland, MA.

Hille, B., A. M. Woodhull, and B. I. Shapiro. 1975. Negative surface charge near sodium channels of nerve: divalent ions, monovalent ions, and pH. *Philosophical Transactions Royal Society of London B.* 270:301–318.

Hodgkin, A. L., and A. F. Huxley. 1952. A quantitative description of membrane current and its application to conduction and excitation in nerve. *Journal of Physiology.* 117:500–544.

Matteson, D. R., and R. P. Swenson, Jr. 1986. External monovalent cations that impede the closing of K channels. *Journal of General Physiology.* 87:795–816.

Miller, C. 1987. Trapping single ions inside single ion channels. *Biophysical Journal.* 52:123–126.

Miller, C., R. Latorre, and I. Reisin. 1987. Coupling of voltage-dependent gating and Ba^{++} block in the high-conductance, Ca^{++}-activated K^+ channel. *Journal of General Physiology.* 90:427–449.

Mozhayeva, G. N., and A. P. Naumov. 1972. Influence of the surface charge on the steady potassium conductivity of the membrane of a node of Ranvier-III. Effects of bivalent cations. *Biofizika.* 17:801–808.

Neyton, J., and C. Miller. 1988*a*. Potassium blocks barium permeation through a calcium-activated potassium channel. *Journal of General Physiology.* 92:549–567.

Neyton, J., and C. Miller. 1988*b*. Discrete Ba^{2+} block as a probe of ion occupancy and pore structure in the high-conductance Ca^{2+}-activated K^+ channel. *Journal of General Physiology.* 92:569–586.

Robbins, J., M. P. Caulfield, H. Higashida, and D. A. Brown. 1991. Genotypic m3-muscarinic receptors preferentially inhibit M-currents in DNA-transfected NG108-15 neuroblastoma x glioma hybrid cells. *European Journal of Neuroscience.* 3:820–824.

Robbins, J., J. Trouslard, S. J. Marsh, and D. A. Brown. 1992. Kinetic and pharmacological properties of the M-current in rodent neuroblastoma X glioma hybrid cells. *Journal of Physiology.* 451:159–185.

Rudy, B. 1988. Diversity and ubiquity of K channels. *Neuroscience.* 25:729–749.

Swenson, R. P., and C. M. Armstrong. 1981. K^+ channel close more slowly in the presence of external K^+ and Rb^+. *Nature.* 291:427–429.

Vergara, C., and R. Latorre. 1983. Kinetics of Ca^{2+}-activated K^+ channels from rabbit muscle incorporated into planar bilayers. Evidence for a Ca^{2+} and Ba^{2+} blockade. *Journal of General Physiology.* 82:543–568.

Woodhull, A. M. 1973. Ionic blockage of sodium channels in nerve. *Journal of General Physiology.* 61:687–708.